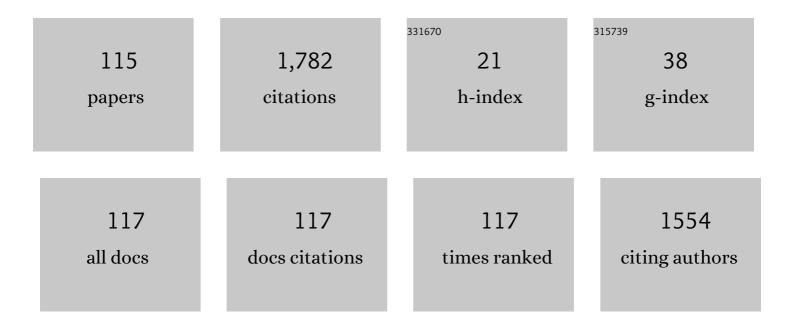
Philippe Leproux

List of Publications by Year in descending order

Source: https://exaly.com/author-pdf/4241263/publications.pdf Version: 2024-02-01



DHILIDDE LEDDOLLY

#	Article	IF	CITATIONS
1	White-light supercontinuum generation in normally dispersive optical fiber using original multi-wavelength pumping system. Optics Express, 2004, 12, 4366.	3.4	159
2	Compact supercontinuum sources and their biomedical applications. Optical Fiber Technology, 2012, 18, 375-378.	2.7	154
3	Spatiotemporal characterization of supercontinuum extending from the visible to the mid-infrared in a multimode graded-index optical fiber. Optics Letters, 2016, 41, 5785.	3.3	107
4	Quantitative CARS Molecular Fingerprinting of Single Living Cells with the Use of the Maximum Entropy Method. Angewandte Chemie - International Edition, 2010, 49, 6773-6777.	13.8	97
5	Ultrabroadband multiplex CARS microspectroscopy and imaging using a subnanosecond supercontinuum light source in the deep near infrared. Optics Letters, 2008, 33, 923.	3.3	74
6	Visible supercontinuum generation controlled by intermodal four-wave mixing in microstructured fiber. Optics Letters, 2007, 32, 2173.	3.3	71
7	Label-free tetra-modal molecular imaging of living cells with CARS, SHG, THG and TSFG (coherent) Tj ETQq1 1 0.	784314 rg 3.4	BT /Overlock 62
8	Modeling and Optimization of Double-Clad Fiber Amplifiers Using Chaotic Propagation of the Pump. Optical Fiber Technology, 2001, 7, 324-339.	2.7	60
9	High spectral power density supercontinuum generation in a nonlinear fiber amplifier. Optics Express, 2007, 15, 11358.	3.4	47
10	Spatial beam self-cleaning and supercontinuum generation with Yb-doped multimode graded-index fiber taper based on accelerating self-imaging and dissipative landscape. Optics Express, 2019, 27, 24018.	3.4	44
11	Observation of Raman Optical Activity by Heterodyne-Detected Polarization-Resolved Coherent Anti-Stokes Raman Scattering. Physical Review Letters, 2012, 109, 083901.	7.8	43
12	Ultra wide band supercontinuum generation in air-silica holey fibers by SHG-induced modulation instabilities. Optics Express, 2005, 13, 7399.	3.4	37
13	Chemical imaging of lipid droplets in muscle tissues using hyperspectral coherent Raman microscopy. Histochemistry and Cell Biology, 2014, 141, 263-273.	1.7	35
14	Ultrabroadband (>2000 cm^â^1) multiplex coherent anti-Stokes Raman scattering spectroscopy using a subnanosecond supercontinuum light source. Optics Letters, 2007, 32, 3050.	3.3	34
15	Hyperspectral coherent Raman imaging – principle, theory, instrumentation, and applications to life sciences. Journal of Raman Spectroscopy, 2016, 47, 116-123.	2.5	32
16	Supercontinuum generation in a nonlinear Yb-doped, double-clad, microstructured fiber. Journal of the Optical Society of America B: Optical Physics, 2007, 24, 788.	2.1	24
17	Nonlinear photonic crystal fiber with a structured multi-component glass core for four-wave mixing and supercontinuum generation. Optics Express, 2009, 17, 15392.	3.4	24
18	SHG-specificity of cellular Rootletin filaments enables naÃ ⁻ ve imaging with universal conservation. Scientific Reports, 2017, 7, 39967.	3.3	24

Philippe Leproux

#	Article	IF	CITATIONS
19	Multiplex coherent anti-Stokes Raman scattering highlights state of chromatin condensation in CH region. Scientific Reports, 2019, 9, 13862.	3.3	24
20	Microstructured fibers with highly nonlinear materials. Optical and Quantum Electronics, 2007, 39, 1057-1069.	3.3	23
21	Invited Article: CARS molecular fingerprinting using sub-100-ps microchip laser source with fiber amplifier. APL Photonics, 2018, 3, .	5.7	22
22	Protein Secondary Structure Imaging with Ultrabroadband Multiplex Coherent Anti-Stokes Raman Scattering (CARS) Microspectroscopy. Journal of Physical Chemistry B, 2012, 116, 1452-1457.	2.6	21
23	Multicolor multiphoton microscopy based on a nanosecond supercontinuum laser source. Journal of Biophotonics, 2016, 9, 709-714.	2.3	21
24	Near-infrared supercontinuum laser beam source in the second and third near-infrared optical windows used to image more deeply through thick tissue as compared with images from a lamp source. Journal of Biomedical Optics, 2015, 20, 030501.	2.6	20
25	Structured-Core GeO\$_{2}\$-Doped Photonic-Crystal Fibers for Parametric and Supercontinuum Generation. IEEE Photonics Technology Letters, 2010, 22, 1259-1261.	2.5	19
26	Characterization of Intra/Extracellular Water States Probed by Ultrabroadband Multiplex Coherent Anti-Stokes Raman Scattering (CARS) Spectroscopic Imaging. Journal of Physical Chemistry A, 2019, 123, 3928-3934.	2.5	19
27	Q-switched Yb-doped nonlinear microstructured fiber laser for the emission of broadband spectrum. Optics Letters, 2007, 32, 3299.	3.3	17
28	Highly germanium and lanthanum modified silica based glasses in microstructured optical fibers for non-linear applications. Optical Materials, 2010, 32, 1002-1006.	3.6	17
29	Blue-Extended Sub-Nanosecond Supercontinuum Generation in Simply Designed Nonlinear Microstructured Optical Fibers. Journal of Lightwave Technology, 2011, 29, 146-152.	4.6	17
30	New opportunities offered by compact subâ€nanosecond supercontinuum sources in ultraâ€broadband multiplex CARS microspectroscopy. Journal of Raman Spectroscopy, 2011, 42, 1871-1874.	2.5	17
31	Raman optical activity spectroscopy by visible-excited coherent anti-Stokes Raman scattering. Optics Letters, 2015, 40, 4170.	3.3	16
32	Identification of intracellular squalene in living algae, <i>Aurantiochytrium mangrovei</i> with hyperâ€spectral coherent antiâ€Stokes Raman microscopy using a subâ€nanosecond supercontinuum laser source. Journal of Raman Spectroscopy, 2017, 48, 8-15.	2.5	16
33	Fast epi-detected broadband multiplex CARS and SHG imaging of mouse skull cells. Biomedical Optics Express, 2018, 9, 245.	2.9	16
34	Ultra-multiplex CARS spectroscopic imaging with 1-millisecond pixel dwell time. OSA Continuum, 2019, 2, 1693.	1.8	16
35	Optical poling in germanium-doped microstructured optical fiber for visible supercontinuum generation. Optics Letters, 2008, 33, 2011.	3.3	15
36	Second and third order susceptibilities mixing for supercontinuum generation and shaping. Optical Fiber Technology, 2012, 18, 283-289.	2.7	15

Philippe Leproux

#	Article	IF	CITATIONS
37	Control of near-infrared supercontinuum bandwidth by adjusting pump pulse duration. Optics Express, 2012, 20, 10750.	3.4	14
38	Surfactant Uptake Dynamics in Mammalian Cells Elucidated with Quantitative Coherent Anti-Stokes Raman Scattering Microspectroscopy. PLoS ONE, 2014, 9, e93401.	2.5	14
39	Linear and nonlinear Raman microspectroscopy: History, instrumentation, and applications. Optical Review, 2014, 21, 752-761.	2.0	13
40	Raman cascade suppression by using wide band parametric conversion in large normal dispersion regime. Optics Express, 2005, 13, 8584.	3.4	12
41	Broadband ultrafast spectroscopy using a photonic crystal fiber: application to the photophysics of malachite green. Optics Express, 2007, 15, 16124.	3.4	12
42	Visible Supercontinuum Generation in Holey Fibers by Dual-Wavelength Subnanosecond Pumping. IEEE Photonics Technology Letters, 2006, 18, 2466-2468.	2.5	11
43	Three-pulse multiplex coherent anti-Stokes/Stokes Raman scattering (CARS/CSRS) microspectroscopy using a white-light laser source. Chemical Physics, 2013, 419, 156-162.	1.9	11
44	Multimodal Imaging of Living Cells with Multiplex Coherent Anti-stokes Raman Scattering (CARS), Third-order Sum Frequency Generation (TSFG) and Two-photon Excitation Fluorescence (TPEF) Using a Nanosecond White-light Laser Source. Analytical Sciences, 2015, 31, 299-305.	1.6	11
45	Multiplex coherent anti-Stokes Raman scattering microspectroscopy detection of lipid droplets in cancer cells expressing TrkB. Scientific Reports, 2020, 10, 16749.	3.3	11
46	Visualizing intra-medulla lipids in human hair using ultra-multiplex CARS, SHG, and THG microscopy. Analyst, The, 2021, 146, 1163-1168.	3.5	11
47	Stable mode-locked operation of a low repetition rate diode-pumped Nd:GdVO4laser by combining quadratic polarisation switching and a semiconductor saturable absorber mirror. Optics Express, 2006, 14, 7093.	3.4	10
48	Controlling intermodal four-wave mixing from the design of microstructured optical fibers. Optics Express, 2008, 16, 21997.	3.4	10
49	Unprecedented Raman cascading and four-wave mixing from second-harmonic generation in optical fiber. Optics Letters, 2010, 35, 145.	3.3	10
50	Picosecond polarized supercontinuum generation controlled by intermodal four-wave mixing for fluorescence lifetime imaging microscopy. Optics Express, 2008, 16, 18844.	3.4	9
51	Nonlinear Pulse Reshaping With Highly Birefringent Photonic Crystal Fiber for OCDMA Receivers. IEEE Photonics Technology Letters, 2010, 22, 1367-1369.	2.5	9
52	Coherent anti-Stokes Raman scattering under electric field stimulation. Physical Review B, 2016, 94, .	3.2	9
53	Modal properties of solid-core photonic bandgap fibers. Photonics and Nanostructures - Fundamentals and Applications, 2006, 4, 116-122.	2.0	8
54	Time-frequency resolved analysis of a nanosecond supercontinuum source dedicated to multiplex CARS application. Optics Express, 2012, 20, 29705.	3.4	8

#	Article	IF	CITATIONS
55	Electronically resonant third-order sum frequency generation spectroscopy using a nanosecond white-light supercontinuum. Optics Express, 2014, 22, 10416.	3.4	8
56	Multimodal and multiplex spectral imaging of rat cornea <i>ex vivo</i> using a whiteâ€light laser source. Journal of Biophotonics, 2015, 8, 705-713.	2.3	8
57	Dynamical study of the water penetration process into a cellulose acetate film studied by coherent anti-Stokes Raman scattering (CARS) microspectroscopy. Chemical Physics Letters, 2016, 655-656, 86-90.	2.6	8
58	Photonic crystal fibres for lasers and amplifiers. Comptes Rendus Physique, 2006, 7, 224-232.	0.9	7
59	Supercontinuum Generation in an Ytterbium-Doped Photonic Crystal Fiber for CARS Spectroscopy. IEEE Photonics Technology Letters, 2016, 28, 2011-2014.	2.5	7
60	Multimodal nonlinear optical imaging of <i>Caenorhabditis elegans</i> with multiplex coherent anti-Stokes Raman scattering, third-harmonic generation, second-harmonic generation, and two-photon excitation fluorescence. Applied Physics Express, 2020, 13, 072002.	2.4	7
61	Labelâ€free detection of polysulfides and glycogen of Cyanidium caldarium using ultraâ€multiplex coherent antiâ€Stokes Raman scattering microspectroscopy. Journal of Raman Spectroscopy, 0, , .	2.5	7
62	Spatial filtering efficiency of single-mode optical fibers for stellar interferometry applications: phenomenological and numerical study. Optics Communications, 2005, 244, 209-217.	2.1	6
63	Theoretical and experimental study of loss at splices between standard single-mode fibres and Er-doped fibres versus direction. Optics Communications, 2000, 174, 419-425.	2.1	5
64	Efficiency of dispersive wave generation in dual concentric core microstructured fiber. Journal of the Optical Society of America B: Optical Physics, 2015, 32, 1676.	2.1	5
65	Visualization of intracellular lipid metabolism in brown adipocytes by time-lapse ultra-multiplex CARS microspectroscopy with an onstage incubator. Journal of Chemical Physics, 2021, 155, 125102.	3.0	5
66	Flow cytometer based on triggered supercontinuum laser illumination. Cytometry Part A: the Journal of the International Society for Analytical Cytology, 2012, 81A, 611-617.	1.5	4
67	Photo-induced meta-stable polar conformations in polystyrene microspheres revealed by time-resolved SHG microscopy. Applied Physics Express, 2020, 13, 052003.	2.4	4
68	Quantitative coherent anti-Stokes Raman scattering microspectroscopy using a nanosecond supercontinuum light source. Optical Fiber Technology, 2012, 18, 388-393.	2.7	3
69	Imaging of tissue using a NIR supercontinuum laser light source with wavelengths in the second and third NIR optical windows. , 2015, , .		3
70	Spectro-temporal shaping of supercontinuum for subnanosecond time-coded M-CARS spectroscopy. Optics Letters, 2016, 41, 5007.	3.3	3
71	Measurement of the third order nonlinear susceptibility of paratellurite single crystal using multiplex CARS. AIP Advances, 2019, 9, 105301.	1.3	3
72	Visualization of water concentration distribution in human skin by ultra-multiplex coherent anti-Stokes Raman scattering (CARS) microscopy. Applied Physics Express, 2021, 14, 042010.	2.4	3

#	Article	IF	CITATIONS
73	Mapping the second and third order nonlinear susceptibilities in a thermally poled microimprinted niobium borophosphate glass. Optical Materials Express, 2021, 11, 3411.	3.0	3
74	Compact sub-nanosecond wideband laser source for biological applications. Applied Physics B: Lasers and Optics, 2007, 86, 601-604.	2.2	2
75	Effect of a Stretching Procedure on the Penetration Process of Water into a Cellulose Acetate Film by Coherent Anti-Stokes Raman Scattering (CARS) Microspectroscopy. Chemistry Letters, 2017, 46, 92-94.	1.3	2
76	Ultrabroadband Multiplex Coherent anti-Stokes Raman Scattering (CARS) Microspectroscopy Using a CCD Camera with an InGaAs Image Intensifier. Chemistry Letters, 2018, 47, 704-707.	1.3	2
77	Second Harmonic Generation in a Highly Birefringent Nonlinear Microstructured Fibre. , 2006, , .		1
78	Discrete spectral selection and wavelength encoding from a visible continuum using optical MEMS. Journal of Micromechanics and Microengineering, 2008, 18, 065010.	2.6	1
79	Methods for visible supercontinuum generation in doped/undoped holey fibres. Proceedings of SPIE, 2008, , .	0.8	1
80	Microstructured fibers with high lanthanum oxide glass core for nonlinear applications. , 2009, , .		1
81	Frequency-dissymmetric parametric sideband generation in a microstructured fiber. Journal of the Optical Society of America B: Optical Physics, 2013, 30, 2889.	2.1	1
82	Imaging microfractures and other abnormalities of bone using a supercontinuum laser source with wavelengths in the four NIR optical windows. Proceedings of SPIE, 2015, , .	0.8	1
83	Multiphoton imaging with a nanosecond supercontinuum source. , 2016, , .		1
84	All-normal dispersion supercontinuum generation in the near-infrared by Raman conversion in standard optical fiber. Proceedings of SPIE, 2016, , .	0.8	1
85	Effect of a Waterproofing Agent on the Penetration Process of Water into a Cellulose Acetate Film by Time-resolved Coherent Anti-Stokes Raman Scattering (CARS) Microspectroscopy. Chemistry Letters, 2017, 46, 833-836.	1.3	1
86	Segmentation integration in multivariate curve resolution applied to coherent anti-Stokes Raman scattering. , 2021, , .		1
87	Intermodal Four-Wave Mixing in Structured-Core Photonic Crystal Fiber: Experimental Results. , 2009, , .		1
88	Toward whole brain label-free molecular imaging with single-cell resolution sing ultra-broadband multiplex CARS microspectroscopy. , 2022, , .		1
89	Multiplex CARS microspectroscopy in the "long-pulse―regime: where are we now?. , 2022, , .		1
90	Dynamics of modulation instability in large normal dispersion regime induced by double wavelength pumping. , 2006, , .		0

6

#	Article	IF	CITATIONS
91	Second and third order nonlinearities in a highly birefringent holey fiber for supercontinuum generation. , 2006, , .		Ο
92	BPM-Numerical Study of Microstructured Fiber With High Difference Index Profile. Journal of Lightwave Technology, 2008, 26, 3261-3268.	4.6	0
93	Second harmonic generation in Ge-doped silica holey fibres and supercontinuum generation. , 2008, , .		Ο
94	Broadband Four-Wave Mixing and Supercontinuum Generation in Multi-Component-Core Photonic Crystal Fiber. , 2009, , .		0
95	Adjustable supercontinuum laser source with low coherence length and low timing jitter. Proceedings of SPIE, 2010, , .	0.8	0
96	Optical continuum generation seeded by stimulated Raman scattering. , 2010, , .		0
97	Quantitative CARS Spectral Imaging of a Single Living Cell in the Fingerprint Region. , 2010, , .		0
98	Experimental study and optimisation of pump laser parameters for supercontinuum generation. , 2011, , .		0
99	Spectro-temporal characterisation of incoherent supercontinuum subnanosecond laser emission for multiplex-CARS microspectroscopy. , 2011, , .		Ο
100	A novel electro-optical pump-probe system for bioelectromagnetic investigations. Proceedings of SPIE, 2012, , .	0.8	0
101	Bright dispersive waves in dual-core microstructured fiber under different laser pumps. , 2013, , .		Ο
102	Frequency-dissymmetric nonlinear sideband generation in a photonic crystal fibre. , 2013, , .		0
103	M-CARS and EFISHG study of the influence of a static electric field on a non-polar molecule. , 2016, , .		Ο
104	Nanosecond coherent anti-Stokes Raman scattering for particle size characterization. Proceedings of SPIE, 2016, , .	0.8	0
105	Measurement of the Third Order Nonlinear Susceptibility of a Paratellurite Single Crystal using Multiplex CARS. , 2019, , .		Ο
106	Versatile supercontinuum generation by using χ(2) and χ(3) nonlinearities in PPLN crystal for direct CARS measurement. , 2021, , .		0
107	Kerr beam self-cleaning and supercontinuum generation in a graded-index few-mode photonic crystal fiber. , 2021, , .		0
108	Adaptive spectral selection of a super continuum source using optical MEMS for biomedical diagnosis. , 2008, , .		0

#	Article	IF	CITATIONS
109	Experimental and numerical investigation of the impact of pulse duration on supercontinuum generation in a photonic crystal fiber. , 2010, , .		О
110	Lasers multicolores pour le diagnostic cellulaire. Photoniques, 2012, , 50-54.	0.1	0
111	Design of an Optimized Distal Optic for Non Linear Endomicroscopy. , 2015, , .		Ο
112	CARS molecular fingerprinting using a sub-nanosecond supercontinuum light source. , 2018, , .		0
113	Label-free imaging of acanthamoeba using multimodal nonlinear optical microscopy. , 2018, , .		Ο
114	χ(3) nonlinear fast imaging and its relative quantification after thermal poling of niobium borophospate glass. , 2020, , .		0
115	Generation of kilovolt, picosecond electric pulses by coherent combining in optoelectronic system. , 2020, , .		0